pubs.acs.org/IC

An Electron-Poor Dioxa-[2.1.1]-(2,6)-pyridinophane Ligand and Its Application in Cu-Catalyzed Olefin Aziridination

Fan Yang, Jiaheng Ruan, Peter Y. Zavalij, and Andrei N. Vedernikov*

Department of Chemistry and Biochemistry, University of Maryland, College Park, Maryland 20742, United States

Supporting Information

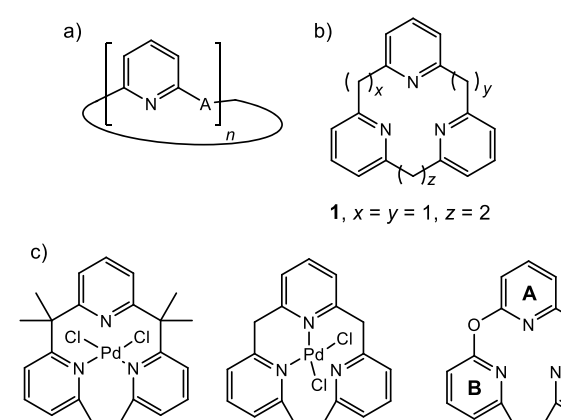
ABSTRACT: A novel macrocyclic 1,7-dioxa-[2.1.1]-(2,6)-pyridinophane ligand has been synthesized and crystallographically characterized. Two derived metal complexes, dichloropalladium(II) and chlorocopper(I), were prepared. In the palladium(II) complex LPdCl₂, both in the solid state, according to its crystallographic characterization, and in CH₂Cl₂ solutions at -40 °C, according to ¹H NMR spectroscopy, the ligand adapts a C_1 -symmetric κ^2 - N_1 Ncoordination mode in which the metal atom binds to two nonequivalent pyridine fragments of the macrocycle. The complex is fluxional at 20 °C. In the crystalline copper(I) complex LCuCl,

the macrocyclic ligand is also κ^2 -N,N-coordinated to the metal, but it utilizes two equivalent pyridine fragments for the binding. The copper(I) complex is fluxional in CH₂Cl₂ solutions in the temperature range between 20 and -70 °C and is proposed to be involved in a fast intermolecular macrocyclic ligand exchange which is slowed down below -40 °C. DFT calculations predict a lower thermodynamic stability of the dioxapyridinophane-derived complexes LPdCl₂ and LCuCl, as compared to their [2.1.1] (2,6)-pyridinophane analogs containing bridging CH2 groups instead of the oxygen atoms. The electron poor dioxapyridinophane chlorocopper(I) complex, in combination with NaBArF₄ (BArF₄ = tetrakis[3,5-bis(trifluoromethyl)phenyl]borate) in dichloromethane solutions, can serve as an efficient catalyst for aziridination of various olefins with PhINTs at 0−22 °C.

INTRODUCTION

(2,6)-Pyridinophanes, macrocyclic (poly)pyridine derivatives (Scheme 1a), can serve as chemically robust polydentate ligands in metal coordination chemistry providing unique environment to the bound metal atoms and capable of affecting dramatically their reactivity. 1-8 Mono-1 and dipyr-

Scheme 1. Some Representative Pyridinophanes and **Derived Metal Complexes**



the most

stable isomer

idine-containing macrocycles (Scheme 1a; n = 1 and 2, respectively) are synthetically the most readily available and have received increased attention as ligands.²⁻⁴ In turn, tripyridine-containing macrocycles, [x.y.z]-(2,6)-pyridinophanes (Scheme 1b) are less explored in this respect. Among the latter, [3.3.3]-(2,6)-pyridinophanes (Scheme 1b, x = y = z= 3) with a larger macrocycle size were found to be a good fit to large lanthanide ions Ln³⁺, whereas [2.1.1]-(2,6)pyridinophanes (Scheme 1b, x = y = 1, z = 2) with a smaller macrocycle size are suitable for metal ions derived from 3d-, 4d-,⁵ and 5d-block^{5,7} elements.

The coordination behavior of parent [2.1.1]-(2,6)-pyridinophane ligand 1 (Scheme 1b) and its derivatives, as well as the reactivity of the derived late d-block metal complexes are influenced strongly by the ligand constrained geometry and the macrocycle size which is slightly larger-than-optimal for the most efficient binding of all three nitrogen donor atoms. 5-7 These properties of 1 impart some lability (κ^3 -coordination) to the derived metal complexes. In particular, the lability of κ^3 coordinated ligand 1 enables facile and reversible alkane and arene C-H oxidative addition/reductive elimination chemistry involving a coordinated PtII/PtIV center. In turn, the metal derivatives containing κ^2 -coordinated ligand 1, such as LPtMe₂ and LPdCl₂, are fluxional at 20 °C, 5 but the increasing ligand

Received: August 30, 2019 Published: November 4, 2019

2. the only

В

Scheme 2. Synthesis of Dioxa-[2.1.1]-(2,6)-pyridinophane 4

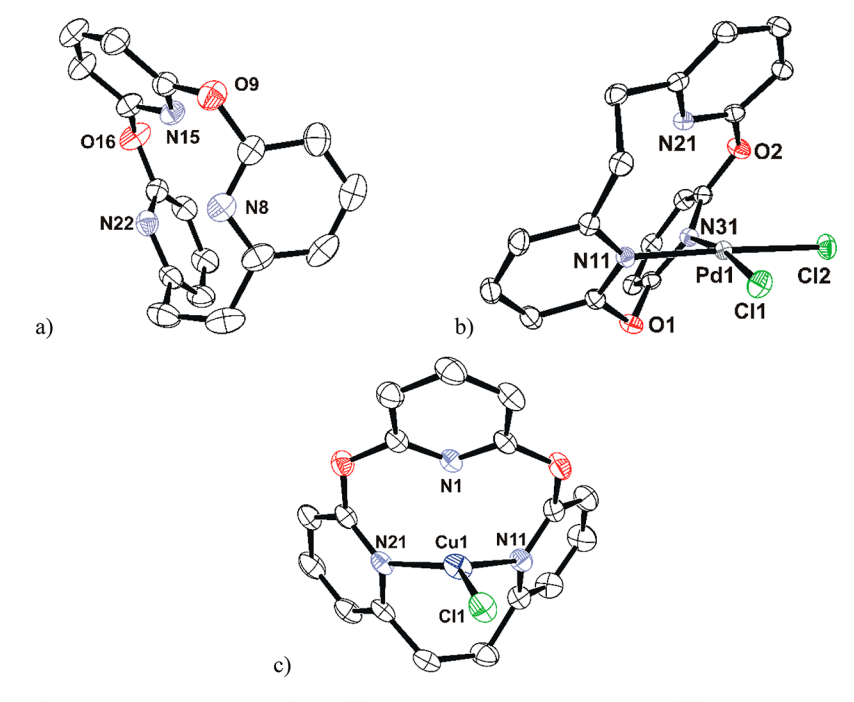


Figure 1. ORTEP drawings (50% probability ellipsoids) for (a) 4 and the derived complexes, (b) dichloropalladium(II) complex 9, and (c) chlorocopper(I) complex 10 (hydrogen atoms are omitted for clarity; solvent molecules are not shown). Selected distances (Å) and angles (degrees) for (b): Pd1-N11, 2.041(1), Pd1-N21, 2.879(1); Pd1-N31, 2.050(1); Pd1-Cl1, 2.278(1); Pd1-Cl2, 2.293(1); N11-Pd1-N31, 83.88(4); N31-Pd1-N21, 66.98(4); N11-Pd1-N21, 80.19(4); N31-Pd1-Cl1, 171.23(3); N31-Pd1-Cl2, 92.25(3); N11-Pd1-Cl1, 91.78(3); N11-Pd1-Cl2, 175.35(3); Cl1-Pd1-Cl2, 91.71(1). Selected distances (Å) and angles (degrees) for (c): Cu1-N11, 2.115(2), Cu1-N21, 2.056(2); Cu1-N1, 2.355(2); Cu1-Cl1, 2.167(1); N11-Cu1-N21, 94.53(6); N11-Cu1-N1, 76.58(6); N21-Cu1-N1, 75.55(6); N21-Cu1-Cl1, 137.00(4); N11-Cu1-Cl1, 123.82(5); N1-Cu1-Cl1, 127.67(4).

steric bulk resulting from methylation of its CH_2 linkers affects the preferred mode of the ligand κ^2 -coordination to Pd^{II} (compare 2 and 3 in Scheme 1c) and shuts down fluxional behavior for bulkier complex 2.

The chemical robustness of 1 was exploited in LCu⁺catalyzed nitrene transfer to olefins⁸ and alkane dehydrogenation/olefin aziridination sequence with PhINTs as a nitrene source. Expectedly, the structural rigidity and chemical reactivity of pyridinophane-supported metal complexes may be modified by replacing the methylene linkers in 1 with other groups, e.g., oxygen atoms, as in dioxa-[2.1.1]-(2,6)-pyridinophane 4. Such structural modification may affect the ligand donicity, making ligand 4 and derived complexes more electron-poor and more chemically robust. Recently, electron-poor tripod ligands were used successfully to generate and characterize some highly reactive terminal copper nitrene complexes, as well as to accomplish a carbene insertion into methane C–H bonds. In turn, the overwhelming majority of

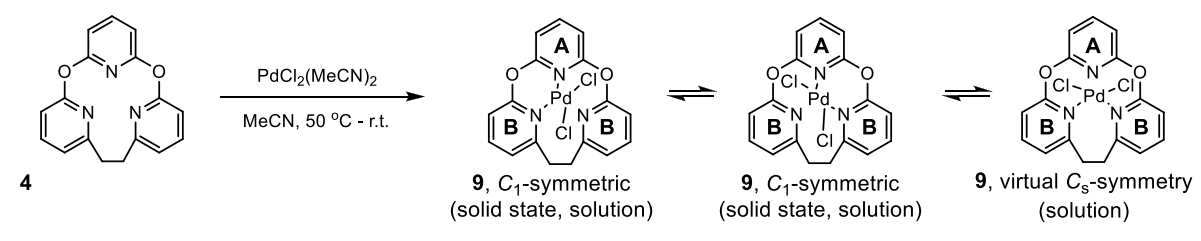
(2,6)-pyridinophane ligands used in coordination chemistry are electron-rich, ¹⁴ and all the previously reported [2.1.1]-(2,6)-pyridinophanes⁵ are not an exception.

In this work, it was our goal to synthesize new dioxa-[2.1.1]-(2,6)-pyridinophane 4, prepare some derived representative dblock metal complexes, and compare their structure and reactivity with those of their analogs derived from the parent ligand 1. A report of this work is presented below.

■ RESULTS AND DISCUSSION

Synthesis of Dioxa-[2.1.1]-(2,6)-pyridinophane 4. New pyridinophane 4 was prepared in an overall 11% yield starting from 2-chloro-6-methylpyridine 5, as shown in Scheme 2. Methylpyridine 5 was lithiated using n-BuLi in THF at -60 °C, and the resulting 6-chloropicolyllithium was subjected to oxidative C–C coupling using 0.5 equiv of 1,2-dibromoethane to produce 1,2-bis(6-chloropyridin-2-yl)ethane 6. A quantitative-by-NMR nucleophilic substitution of chlorine atoms in 6

Scheme 3. Synthesis of Dichloropalladium(II) complex 9



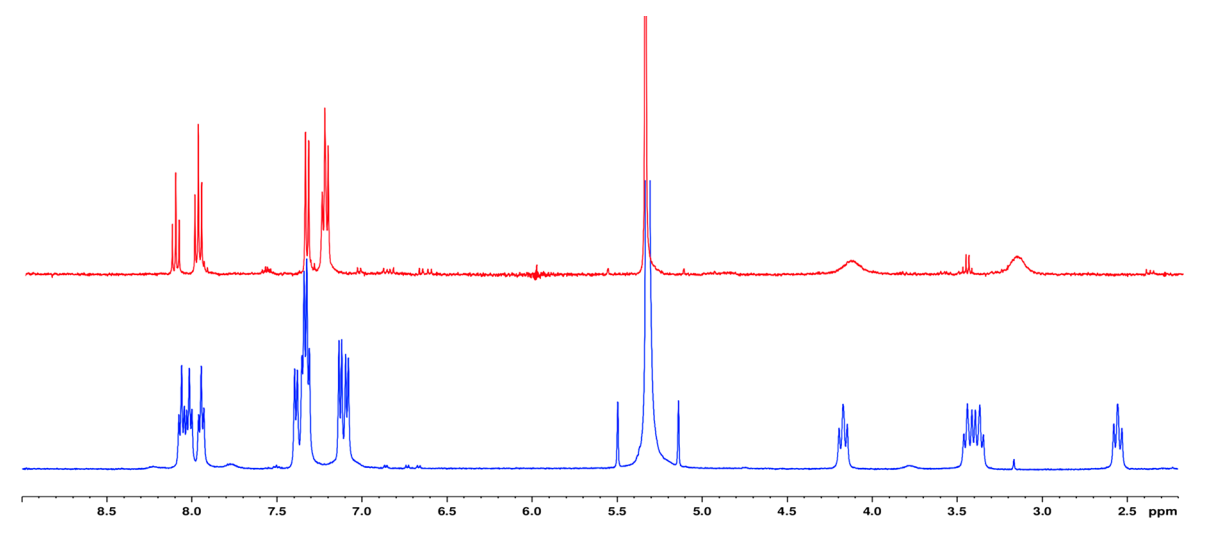


Figure 2. ¹H NMR spectra of complex 9 in CD₂Cl₂ at 22 °C (top) and -40 °C (bottom).

with OH groups occurred after heating **6** with aqueous hydrochloric acid at 170 °C for 2 days. The resulting bispyridinol was isolated as HCl salt 7. Deprotonation of 7 with *n*-BuLi in ether led to dilithium derivative **8** which was reacted with 2,6-dichloropyridine in 1,3-dimethyl-2-imidazolidinone (DMI) solvent to form **4**. Single crystals of macrocycle **4** were produced upon its recrystallization from ethyl acetate and were characterized by X-ray diffraction analysis (Figure 1a).

Similar to the CH₂- and CMe₂-bridged [2.1.1]-(2,6)-pyridinophanes,⁵ macrocycle 4 adapts an "alternate cone"-type arrangement of the three pyridine rings, allowing it to avoid an accommodation of three nitrogen lone pairs in a close proximity of each other, so minimizing their mutual repulsion. An additional factor favoring the outward orientation of the symmetry-unique pyridine ring **A** in macrocycle 4 (see Scheme 1) may be some weak stabilizing $n(O)-\pi^*(py)$ interaction between nonbonding orbitals of the bridging oxygen atoms and the π^* -orbitals of pyridine ring **A**. Because of this stabilizing orbital interaction, 4 may be less prone to adapt a "cone" geometry necessary for the facial κ^3 - N_1 , N_2 -coordination to a metal center.

Preparation, Structural Characterization, and Fluxional Behavior of Dichloropalladium(II) Complex 9. Mixing 4 with PdCl₂(MeCN)₂ dissolved in acetonitrile at 50 °C with subsequent cooling of the mixture to room temperature and crystallization overnight produces pure dichloropalladium(II) complex 9 as an orange powder (Scheme 3).

Single crystals of 9 could be grown from its saturated dichloromethane solution layered with pentanes. According to X-ray diffraction analysis of 9 (Figure 1b), the complex is C_1 -symmetric in the solid state. The palladium atom coordination geometry is a slightly distorted square planar. The macrocyclic

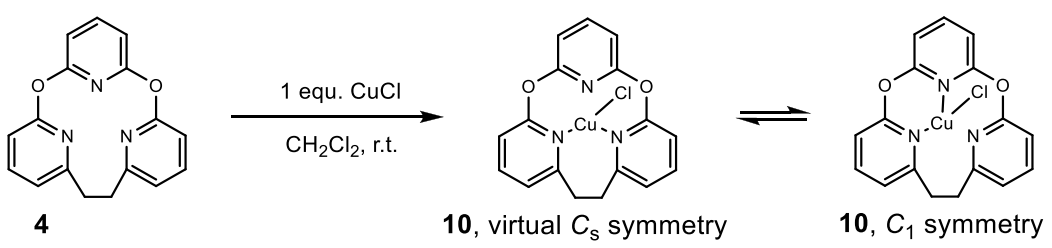
ligand in 9 adapts a κ^2 -N₁N-coordination mode utilizing nitrogen donor atoms of two nonequivalent pyridine rings, A and B (Scheme 1c), where the Pd1-N31 (ring A) distance, 2.050(1) Å, is slightly longer than the Pd1-N11 (ring B) distance, 2.041(1) Å. The third pyridine ring of the coordinated macrocycle assumes an outward orientation of its nitrogen lone pair with the Pd1-N21 distance of 2.879(1) Å to minimize the repulsion between the nitrogen lone pair and nonbonding electron pairs of the metal occupying its d_{z^2} , d_{xy} , and d_{yz} orbitals. The orientation of the pendant pyridine ring is similar, in a related structurally characterized complex 2 (Scheme 1c) having bridging CMe2 groups. 5a In contrast to our new complex 9, complex 2 has an idealized C_s-symmetric structure allowing the metal atom to minimize another type of destabilizing repulsive interactions, not present in 9 and involving the ligand methyl groups situated in the close proximity to the metal.

NMR characterization of 9 was performed in CD₂Cl₂ solutions. Due to low solubility of 9 in most common solvents, the characterization was limited to ¹H NMR spectroscopy. The ¹H NMR spectrum of 9 recorded at 22 °C exhibits a pattern typical for an apparent C_s-symmetric complex with five sharp partially overlapping multiplets in the aromatic region (Figure 2, top), and the C₂H₄ linker protons give rise to two broad signals. These observations suggest a fluxional behavior of 9, which was also documented for parent CH2-bridged complex 3 (Scheme 1c) in the same solvent. 5a The 1H NMR spectrum of 9 recorded at -40 °C (Figure 2, bottom) shows six sharp essentially resolved and one unresolved multiplet in the aromatic region along with two sharp well-resolved and two overlapping multiplets of the C₂H₄ linker protons. The observed low-temperature spectrum is consistent with the realization of two enantiomeric C_1 -symmetric structures of 9

Scheme 4. DFT-Calculated Gibbs Energy of an Imaginary Pyridinophane Ligand Exchange Reaction Involving Complexes 3 and 9 and Ligands 1 and 4^a

^aConditions: CH₂Cl₂, 25 °C.

Scheme 5. Synthesis of Chlorocopper(I) Complex 10



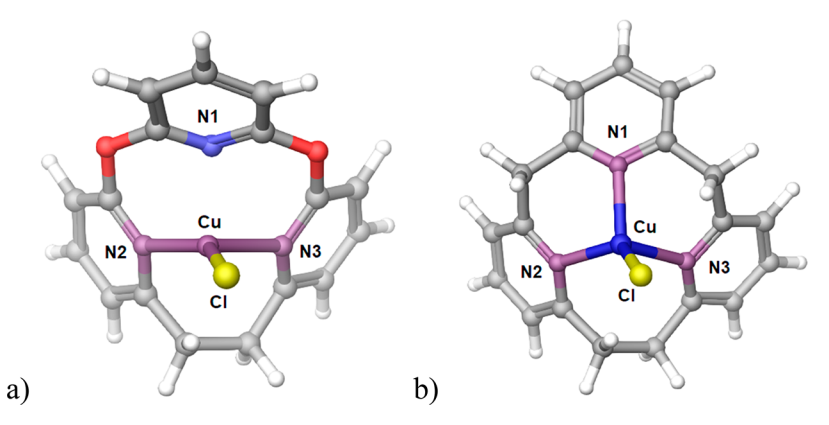


Figure 3. DFT-optimized geometries of 10 (a) and 11 (b). Selected distances (Å) and bond angles (degrees): (a) 10, Cu-N1, 2.37; Cu-N2, 2.06; Cu-N3, 2.28; N2-Cu-N3, 90.2; N2-Cu-Cl, 143.7; N3-Cu-Cl, 121.4; (b) 11, Cu-N1, 2.04; Cu-N2, 2.06; Cu-N3, 2.16; N2-Cu-N3, 100.9; N2-Cu-Cl, 129.3; N3-Cu-Cl, 109.9; N1-Cu-N2, 92.2; N1-Cu-N3, 93.2.

(Scheme 3), also found in the solid state (Figure 1b). At 20 $^{\circ}$ C the enantiomers and an additional C_s -symmetric isomer are involved in an interconversion with a fast migration of the metal atom between three pyridine rings of the macrocycle.

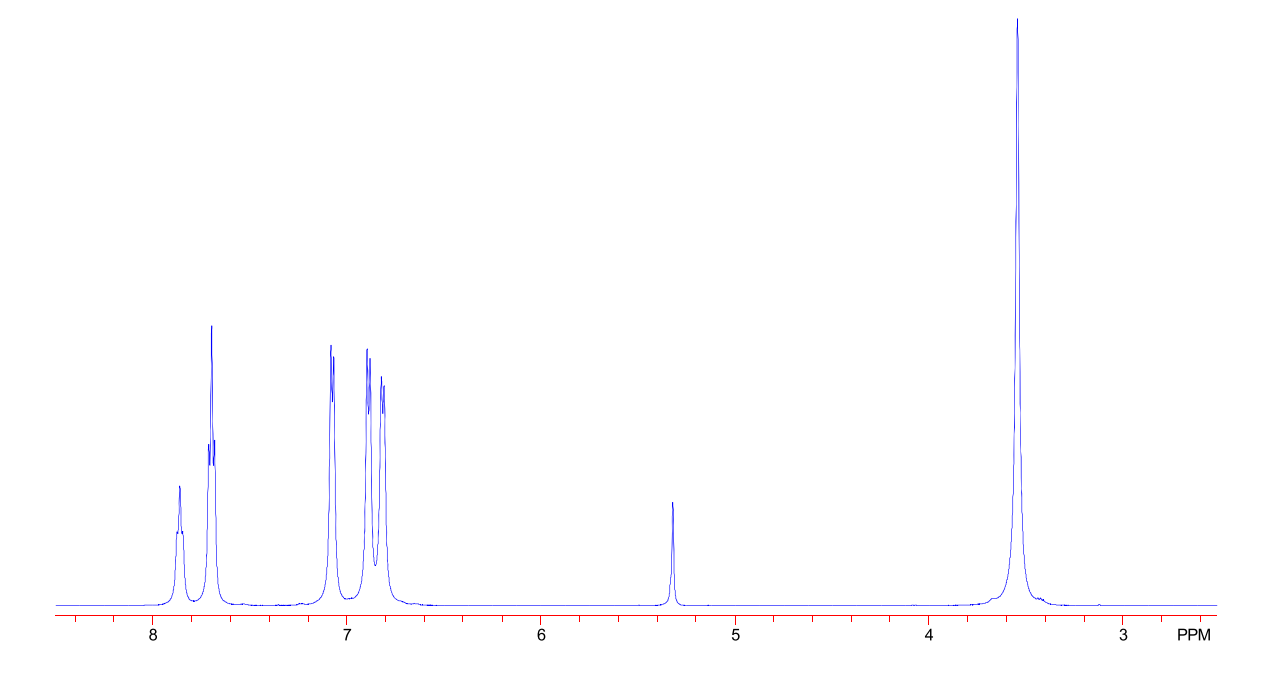
The relative stabilities of the C_1 - and C_s -symmetric isomers of 9 were estimated using DFT calculations. The calculations show that these isomers are almost equally stable at 25 °C, with the Gibbs energy of the latter being only 0.1 kcal/mol higher. This is a significant change from the 7.1 kcal/mol difference between the more stable C₁-symmetric isomer and the less stable C_s -symmetric isomer of 3. The most likely cause of this change involves two factors. As compared to the C₁symmetric isomers of 3 and 9, their C_s -symmetric counterparts experience stronger repulsion between the metal lone pairs occupying its d_{z^2} orbital and π -electrons of the pendant pyridine ring. This is because the linkers holding the pendant pyridine rings in the C_s -symmetric species, two CH_2 groups in 3 or two O atoms in 9, are shorter overall, as compared to their C_1 -symmetric counterparts where one of the linkers is the longer ethylene tether. However, the C_1 -symmetric isomer of 9 may be slightly destabilized because the metal atom here is

coordinated to an electron-poorest ring, A (Scheme 3), having two electron-withdrawing oxygen substituents.

To compare the overall binding energy of macrocyclic ligands 1 and 4 to that of the $Pd^{II}Cl_2$ fragment, we used DFT calculations. The imaginary pyridinophane ligand exchange reaction involving complexes 3 and 9 and macrocycles 1 and 4 (Scheme 4) shows a dramatic preference, by 17.4 kcal/mol in the Gibbs energy scale, for the $Pd^{II}Cl_2$ fragment coordination to electron-richer methylene-bridged ligand 1.

Hence, overall, 4 is a poorer electron donor, as compared to 1. The replacement of two methylene linkers in pyridinophane complex 3 with two oxo groups in 9 diminishes significantly the thermodynamic stability of the derived dichloropalladium-(II) complexes. In turn, the reason behind the lower donicity of 4 appears to be the electron-withdrawing character of two bridging oxygen atoms. In support to this claim, the average energy of three ligand 4 molecular orbitals accommodating its nitrogen donor atoms lone pairs is -5.56 eV, as compared to -5.16 eV for CH₂-bridged parent compound 1 (Table S1).

Preparation and Characterization of Chlorocopper(I) Complex 10. The chorocopper(I) complex derived from dioxapyridinophane 4 was prepared by stirring CuCl with 1



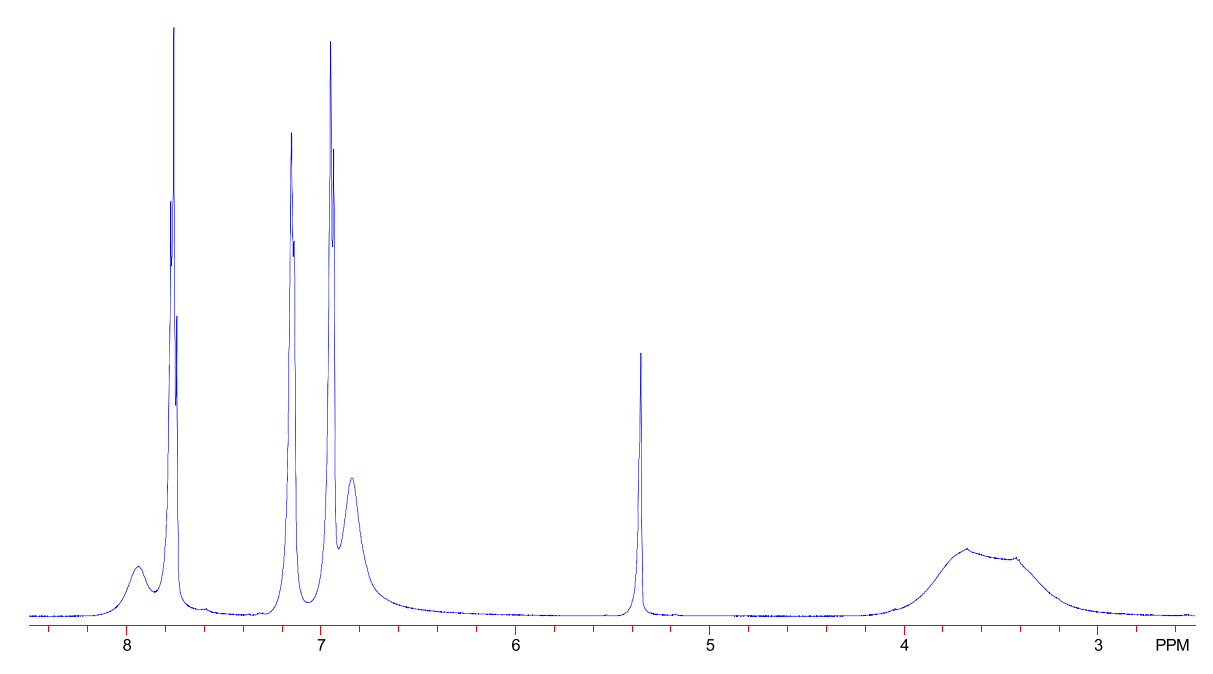


Figure 4. ¹H NMR spectrum of complex 10 in CD₂Cl₂ at 20 °C (top) and -40 °C (bottom).

equiv of 4 dissolved in dichloromethane at room temperature (Scheme 5). The reaction was complete after 10 min to give a pale yellow solution of target compound 10.

Single crystals of 10 suitable for X-ray diffraction analysis were grown from its dichloromethane solution layered with cyclooctane. According to crystallographic characterization (Figure 1c), the pyridinophane ligand is κ^2 -N,N-coordinated to the metal and utilizes two nitrogen donor atoms of two equivalent pyridine fragments, **B** (Scheme 1c). The structure of 10 can be viewed as a result of a distortion of a C_s -symmetric species that allows the ethylene linker C_2H_4 to assume a staggered conformation. The copper atom coordination geometry is distorted trigonal planar with the metal atom

slightly deviating from the plane of the three attached donor atoms, N11, N21, and Cl1. The sum of the three adjacent angles, N21–Cu1–Cl1, N11–Cu1–Cl1, and N21–Cu1–N11, is 355.4°. As a result of the distortion, the Cu1–N11 distance, 2.115(2) Å, is longer than the Cu1–N21 distance, 2.056(2) Å. The third, symmetry-unique pyridine ring, A, of the macrocycle is pointing its nitrogen donor lone pair away from the metal with the Cu1–N1 distance of 2.355(2) Å. A comparison of the solid state structure of 10 (Figure 1c) and the DFT-calculated structure of 10 (Figure 3a) shows a good match of the key geometric parameters of the metal coordination unit in the DFT-calculated structure and the solid-state structure.

Scheme 6. Proposed Macrocyclic Ligand Exchange Mechanism in CH_2Cl_2 Solutions of 10 along with DFT-Calculated Reaction Gibbs Energies (kcal) at 25 $^{\circ}C$

Similar to the results of the solid-state structure analysis, both 13 C and 1 H NMR spectra of **10** in CD₂Cl₂ solutions recorded at 22 $^{\circ}$ C show the presence of a single species of a virtual C_s symmetry. The 1 H NMR spectrum of **10** features a slightly broadened singlet at 3.54 ppm corresponding to the protons of the C₂H₄ bridge of ligand **4**, along with five well-resolved multiplets, two triplets, and three doublets, in the aromatic region (Figure 4, top). These signals are noticeably downfield-shifted, as compared to the spectrum of free ligand **4**

The unusual appearance of the signal of the C₂H₄ bridge protons as a relatively narrow singlet with the half-width 10 Hz (Figure 4, top) may suggest a rapid and reversible dissociation of the macrocyclic ligand and/or a rapid intermolecular transfer of the Cu^ICl fragment between different pyridinophane ligands, possibly, via dinuclear pyridinophane-bridged species 12 (Scheme 6, vide infra). In accordance with this hypothesis, the ¹H NMR spectrum of 10 recorded at -40 °C (Figure 4, bottom) shows the C₂H₄ bridge proton signals as two broad unresolved multiplets of approximately equal intensity. The signals of pyridine ring A protons become broad, while the signals originating from apparently equivalent pyridine rings B remain sharp. At -70 °C, the C₂H₄ bridge protons produce two resolved signals of equal intensity; all the signals in the aromatic region become broad and the presence of one more minor species (~15%) becomes apparent (Figure S3). These spectral changes may be associated with a slowing down of an intermolecular Cu^ICl fragment transfer between different pyridinophane ligands shown in Scheme 6.

The experimental observations above have been complemented by DFT calculations (Figure S4). According to the DFT, the lowest-energy structure of 10 (Figure 3a) having the C_2H_4 linker of the pyridinophane ligand in a staggered conformation can interconvert readily into its enantiomer with a calculated Gibbs activation energy of 3.1 kcal/mol. The facile isomerization is responsible for making pyridine rings **B**

equivalent in the NMR time scale at -40 °C. In addition, similar to Pd^{II}Cl₂ complex 9, complex 10 can exist as a C₁symmetric κ^2 -N,N-coordinated isomer with two nonequivalent pyridine fragments, A and B (Scheme 1c), attached to the metal (Scheme 5). These isomers can be involved in another fast interconversion equilibrium. The C_1 -symmetric complex is calculated to be 3.0 kcal/mol higher in energy and is produced from the lowest energy structure with the Gibbs activation energy of 5.4 kcal/mol (Figure S4, TS_{10,uns}). The N1-Cu1 distance in corresponding transition state TS_{10,uns} is relatively long, 2.27 Å, and more importantly, the N1 nitrogen lone pair is still pointing away from the metal atom, suggesting only a weak possible metal-donor interaction. Hence, it may be expected, that the main contribution to the 5.4 kcal/mol activation barrier is associated with the macrocycle conformation change involving reorientation of symmetry-unique pyridine fragment A from "away from the metal" to "pointing to the metal". Comparing the conformational flexibility of 4 and other pyridinophanes in their derived complexes, it is worth noting that ligand 4 in 10 is more "flexible" than a coordinated diazapyridinophane present in Pd(II) complex 13 (Scheme 7) which was studied in detail previously. 15 The height of the barrier associated with the macrocycle η^2 - η^3 rearrangement in 13, 14.9 ± 0.2 kcal/mol, is greater than 5.4 kcal/mol for complex 10 isomerization (Figure S4, TS_{10,uns}).

The proposed mechanism for an intermolecular Cu^1Cl fragment exchange between different macrocyclic ligands has also been analyzed using DFT calculations (Scheme 6, Figure S4). The reaction was proposed to involve a κ^1 -N-coordinated C_1 -symmetric isomer of 10 which is only 4.8 kcal/mol less stable than the ground-state structure. Owing to the fact that in the κ^1 -N-coordinated structure, rings **B** have an opposite orientation of their nitrogen lone pairs, two such species may be involved in a bimolecular transfer of one CuCl moiety resulting in the formation of dinuclear complex 11/free ligand 4 pair with the overall Gibbs energy change of 10.8 kcal/mol.

Scheme 7. η^2 - η^3 -Rearrangement of 2,11-Diaza[3.3]-(2,6)-pyridinophane Ligand in Dichloropalladium(Ii) Complex 13^{15}

$$t$$
-Bu t -Bu

Since two CuCl moieties in 11 are attached to the opposing sides of the macrocyclic ligand, removal of one of them can lead to a virtual "migration" of a $Cu^{I}Cl$ fragment from one face of the macrocycle to another resulting in an NMR-equivalence of the C_2H_4 bridge protons observed at 20 °C.

When discussing structure and dynamics of our new complex 10, it may also be interesting to compare it with its analog, 11 (Figure 3b), containing two CH₂ bridges in the macrocycle instead of two oxygen atoms. First, in contrast to 10, the macrocycle in 11 is κ^3 -coordinated, according to single-crystal X-ray diffraction analysis. Accordingly, H NMR spectra of 11 in CH₂Cl₂ exhibit five sharp multiplets in the aromatic region both at 22 and -45 °C, suggesting a virtual C_s symmetry of 11 at 22 °C, similar to that of 10. In contrast to 10, the C₂H₄ bridge protons of the macrocycle in 11 show two well-resolved multiplets, excluding the possibility of the Cu¹Cl fragment transfer between pyridinophane ligands in CH₂Cl₂ solutions of 11. This pattern can be viewed as a result of a stronger metal—ligand coordination in 11, as compared to that in 10

The weaker metal—macrocyclic ligand binding in **10**, as compared to **11**, could also be demonstrated using DFT calculations. The calculated Gibbs energy of substitution of macrocycle **1** for **4** in complex **10** is -14.6 kcal/mol (Scheme 8), close to the value found for the PdCl₂ fragment transfer reaction in Scheme 4. A particularly low donicity of pyridine fragment **A** in dioxa-pyridinophane **4** appears to be responsible for the lower stability of the C_1 -symmetric versus C_s -symmetric structure of **10**.

Hence, similar to a Pd^{II} coordination, dioxapyridinophane ligand 4, as compared to 1, is also more weakly binding to a Cu^{I} center. This weak coordination enables proposed unusual ligand 4 transfer between Cu^{I} centers affecting the appearance of ^{I}H NMR spectra of derived complex 10.

Attempted Preparation of Platinum(II) Complexes of 4. Holding in mind weak donor properties of 4 one can expect

that preparation of some of its metal derivatives may be problematic. In fact, our attempts to prepare a Pt^{II} analog of complex 9 (Scheme 3) by reacting K_2PtCl_4 and 4 in water were not successful. No changes in the composition of the mixtures were seen by NMR after 2 days. Similarly, no reaction was observed in mixtures of 4 and $Pt_2Me_4(SMe_2)_2$ dissolved in THF after 1 day.

Aziridination of Olefins with PhINTs Catalyzed by 10/ NaBAr^F₄ in Dichloromethane Solutions. The electron-poor nature of ligand 4 may be beneficial when it comes to utilization of some of derived metal complexes in strongly oxidizing conditions such as nitrene transfer. Having an electron-poor metal fragment attached to a nitrene may help maintain the electrophilicity and reactivity of the nitrene on a high level, ¹² allowing for potentially more efficient nitrene transfer catalysis.

In this work we probed the catalytic activity of copper(I) complex 10 in combination with equimolar amounts of NaBAr $_4$ (BAr $_4$ = tetrakis[3,5-bis(trifluoromethyl)phenyl]-borate) acting as a chloride ligand abstractor in dichloromethane solutions in aziridination of various olefins (3–5 equiv) with PhINTs at 0–22 °C (Table 1). As discussed

Table 1. Catalytic Aziridination of Selected Olefins (3–5 equiv) with PhINTs in the Presence of x mol % of 10 and x mol % NaBAr $_4$ (x = 2.5 and 5) in Dichloromethane Solutions at 0 °C

entry	substrate (equiv)	catalyst loading $(x \%)$	aziridine, % yield
1	sis avalonatomo 2	5.0	14, 98 ^a
2	cis-cyclooctene, 3	2.5	14, 90 ^a
3	cis-cycloheptene, 3	2.5	15 , 90
4	cyclohexene, 5	5.0	16 , 80
5	cyclopentene, 5	5.0	17, 78
6	styrene, 3	5.0	18 , 98
7	2-methylbutene, 5	5.0	19 , 98
8	2,3-dimethylbutene, 5	5.0	20 , 98
9	methyl acrylate, 5	5.0	21, 98
10	methyl methacrylate, 5	5.0	22 , 98
11	3,3-dimethylbutene, 5	5.0	23 , 65
12	4,4-dimethylpentene, 5	5.0	24 , 82
13	methyl methacrylate, 5	5.0 ^b	22 , 66
			_

^aReaction run at 22 °C. ^bCatalyst 10 was used without NaBAr^F₄.

earlier,¹⁶ we assume that the metal atom in a catalyst must coordinate PhINTs to produce a reactive nitrene Cu complex.

Scheme 8. DFT-Calculated Gibbs Energy for a Pyridinophane Ligand Exchange Reaction Involving Complexes 10 and 11 and Ligands 1 and 4 in CH_2Cl_2 at 25 $^{\circ}C$

 $\Delta G_{298}^{0} = -14.6 \text{ kcal/mol}$

In the presence of NaBAr^F₄, the chloride ligand present in LCuCl may be abstracted to produce LCu⁺ and a CH₂Cl₂-insoluble NaCl. The cationic species LCu⁺ is more coordinatively unsaturated, less sterically encumbered and more electrophilic than LCuCl. For all these reasons, LCu⁺ is expected to bind PhINTs more readily and allow for faster catalysis. In fact, such reactivity difference was observed in our experiments (*vide infra*).

The CH₂-bridged analog of **10**, complex **11**, has been characterized by us in olefin aziridination previously. The derived catalyst, **11** + NaBAr^F₄, was shown to be highly active in dichloromethane solutions although it underwent a fast degradation producing pale-yellow catalytically inactive species. Hence, it was of our interest to test the catalytic properties of the electron-poorer catalyst derived from **10**. The results of our tests are given in Table 1. Most of the reactions were run at 0–22 °C. Upon addition of a catalyst solution, **10** + NaBAr^F₄ in dichloromethane, to a suspension of PhINTs and 3–5 equiv of olefin dissolved in dichloromethane, the color of the mixture changed to a deep green. Upon stirring for 5–15 min at 0–22 °C, all the PhINTs reagent dissolved.

With 5 mol % catalyst loading, the observed NMR yields of the resulting aziridines, in most cases, are high, in the range of 78-98%. The highest yields were achieved with sterically unhindered olefins where side reactions with nitrene are least likely, 98% for cis-cyclooctene (entry 1), styrene (entry 6), trimethylethylene (entry 7), tetramethylethylene (entry 8), methyl acrylate (entry 9), and methyl methacrylate (entry 10). When the catalyst loading is decreased to 2.5 mol %, the yields decrease slightly (e.g., compare entries 1 and 2). Overall, this level of catalytic activity matches well that of CH2-bridged analog 11 under similar conditions.8 Somewhat lower aziridine yields with 10 as a catalyst are observed for sterically bulkier substrates, tert-butylethylene (65%, entry 11) and neopentylethylene (82%, entry 12). Notably, when complex 10 was used as a catalyst by itself, in the absence of NaBArF4, the aziridine yields are lower, e.g., 66 versus 98%, for methyl methacrylate substrate (entries 13 and 10, respectively).

The most notable result in Table 1 that distinguishes catalysts 10 and 11 in their performance in olefin aziridination concerns reactions of more challenging substrates, the virtually unstrained cycloolefins, cyclohexane (80%, entry 4) and cyclopentene (78%, entry 5). These olefins can also undergo a competitive nitrene insertion into their allylic CH bonds. Notably, using electron-richer and less chemically robust precatalyst 11 with these substrates affords 20–40% lower yields of derived aziridines.

When analyzing the catalytic activity of our 10/NaBArF4 catalyst, it may be interesting to compare it with that of other Cu-based catalysts, although such data available in literature is limited. For a comparison of Cu-catalyzed olefin aziridination with PhINTs, we considered methyl methacrylate as a substrate. Table 2 lists results produced when different catalysts are used in this reaction. The results are arranged in the order of increasing olefin/PhINTs ratio. The higher ratios, in general, favor higher aziridine yields. As it can be seen from Table 2, the yields range between 58 and 98% with the reaction time between 24 h and 10 min. Overall, the performance of our 10 + NaBAr^F₄ catalyst showing 98% yield of the aziridine after 5−15 min of reaction (Table 1, entry 10) compares favorably to that for the rest of the systems. Hence, the new catalytic system based on 10 + NaBAr^F₄ is one of the fastest and high-yielding which may prompt us to pursue

Table 2. Catalytic Aziridination of Methyl Methacrylate with PhINTs and Different Copper-Based Catalysts

olefin/PhINTs molar ratio	catalyst, mol %/solvent, temperature, time	aziridine yield (%)	ref
1:1.2	Cu(OTf) ₂ , 10%/MeCN, 20 °C, 24 h	58	17
1:1.2	Cu(OTf) ₂ , 10%/MeCN, mol. sieves, 20 °C, overnight	68	18
1:1	CuCl ₂ (py) ₂ , 5%/CHCl ₃ , 23 °C, 5 min	72	16
5:1	[Cu(MeCN) ₆][Al{OC(CF ₃) ₃ } ₄] ₂ , 1%/MeCN, 20 min, 25 °C	96	19
5:1	5% 11 + 5% NaBAr ^F ₄ /CH ₂ Cl ₂ , 0 °C, 10 min	98	8

a more detailed future investigation of the catalytic activity of 10 in olefin aziridination.

■ EXPERIMENTAL SECTION

Computational Details. Theoretical calculations in this work have been performed using the density functional theory (DFT) method, 20 specifically functional PBE, 21 and LACVP relativistic basis set with two polarization functions, as implemented in the Jaguar program package.²² Full geometry optimization has been performed without constraints on symmetry in gas phase. The solvation Gibbs energies, G_{solv} in CH_2Cl_2 as solvent were found using single-point calculations utilizing Poisson-Boltzmann continuum solvation model (PBF).²² For all species under investigation frequency analysis has been carried out. All energy minima have been checked for the absence of imaginary frequencies. All transition states possessed just one imaginary frequency. Using the method of intrinsic reaction coordinate, reactants, products, and the corresponding transition states were proved connected by a single minimal energy reaction path. The total gas phase Gibbs free energy ($G_{\rm tot}$) at 298 K were produced in Hartrees (1 hartree = 627.51 kcal/mol). The dispersioncorrected values of the total gas phase Gibbs free energies $(G_{tot D3})$ were found using single point calculations with PBE-D3 functional and the difference of the SCF energies produced with the PBE and PBE-D3 functionals, DFT(pbe) and DFT(pbe-d3):

$$(G_{tot,D3}) = (G_{tot}) - DFT(pbe) + DFT(pbe-d3)$$

Finally, the standard reaction Gibbs energies, $\Delta G_{\rm rxn}$, in kcal/mol were calculated as follows:

$$\begin{split} \Delta G_{\rm rxn} &= 627.51 [\Sigma (G_{\rm tot,D3})_{\rm products} - \Sigma (G_{\rm tot,D3})_{\rm reactants}]_{\rm gas_phase} \\ &+ \Sigma (G_{\rm solv})_{\rm products} - \Sigma (G_{\rm solv})_{\rm reactants} + \Delta nRT \ln (RT/P) \end{split}$$

where Δn is the change in the number of moles in a balanced reaction equation when going from reactants to products. The standard state for all solutes is 1 M concentration.

Preparation of Dioxa-[2.1.1]-(2,6)-pyridinophane, 4. 1,2-Bis(6-chloropyridin-2-yl)ethane, 6. An oven-dried 250 mL round-bottomed flask was charged with a magnetic stir bar under argon atmosphere. The flask was capped, and 150 mL of anhydrous THF and 15 mL (0.15 mol) of anhydrous 6-chloro-2-picoline were introduced. The stirred solution was cooled to −60 °C, and 13.7 mL of a 11.0 M n-butyllithium in hexanes (0.15 mol) was added with a syringe over 20 min. The resulting dark red mixture was stirred at −60 °C for 1 additional hour before being further cooled to −78 °C. A solution of 6.5 mL (0.075 mol) of 1,2-dibromoethane in 10 mL of THF was then injected with a syringe over 10−20 min. When the addition was complete, the light red mixture was allowed to warm up to room temperature overnight resulting in a colorless solution. A saturated aqueous solution of potassium hydroxide (20 g) was added to the reaction to precipitate most of the lithium and bromide ions

and the mixture was swirled thoroughly. The resulting colorless liquid was decanted from a precipitate of lithium hydroxide and potassium bromide and dried overnight over solid potassium hydroxide. After removal of the solvent and distillation under vacuum, pure 1,2-bis(6-chloropyridin-2-yl)ethane was obtained as a colorless crystalline solid. Yield: 13.7 g, 93%. ¹H NMR (400 MHz, CDCl₃, 22 °C), δ : 7.52 (t, J = 7.7 Hz, 2H), 7.15 (dd, J = 7.9, 0.9 Hz, 2H), 7.05 (dd, J = 7.6, 0.9 Hz, 2H), 3.20 (s, 4H). ESI-MS Calcd for $C_{12}H_{11}Cl_2N_2^+$ [M + H]⁺ 252.02. Found: 252.04.

1,2-Bis(6-hydroxypyridin-2-yl)ethane bis(hydrogen chloride), 7. First, 6.6 g of 1,2-bis(6-chloropyridin-2-yl)ethane 6 was dissolved in 25 mL of 30% aqueous HCl. The mixture was transferred to a 50 mL Schlenk tube and sealed. The reaction was heated in silicon oil bath at 170 °C for 40 h. During the first 10 h of reaction, every 2 h, the Schlenk tube was removed from oil bath, cooled to room temperature, and carefully opened to release the pressure of HCl produced in the reaction. After the first 10 h of reaction the pressure was released every 5 h. After 40 h of heating the reaction was cooled to room temperature and transferred to a round-bottomed flask. The excess HCl was removed on a rotavap and the residue was dried under high vacuum to give 7 quantitatively as an off-white crystalline solid, which was used in next step without further purification. ¹H NMR (400 MHz, CD₃OD, 22 °C), δ : 8.16 (dd, J = 8.8, 7.4 Hz, 2H), 7.10 (d, J = 7.4 Hz, 2H), 7.06 (d, J = 8.8 Hz, 2H), 3.28 (s, 4H). ¹³C NMR (151 MHz, CD₃OD, 22 °C), δ: 163.12, 151.26, 116.20, 113.51, 32.48. ESI-MS Calcd for $C_{12}H_{13}N_2O_2^+$ [M + H]⁺ 217.10. Found: 217.14.

Lithium 6,6'-(Ethane-1,2-diyl)bis(pyridin-2-olate), **8**. An ovendried 500 mL round-bottomed flask was charged under argon atmosphere with a stir bar, 7.18 g (33 mmol) of compound 7 and 200 mL of anhydrous diethyl ether. Then, 3.0 mL of a 11.0 M n-butyllithium solution in hexanes was injected to the resulting suspension via syringe. The reaction was stirred under argon for 1 week. The solvent was then carefully removed on a rotavap, and the residue was dried under high vacuum to afford the product **8** in quantitative yield as fine white powder. 1 H NMR (400 MHz, CD₃OD, 22 °C), δ : 7.26 (dd, J = 8.5, 7.0 Hz, 2H), 6.23 (td, J = 8.2, 0.9 Hz, 4H), 2.82 (s, 4H).

[2.1.1]-(2,6)-9,16-Dioxapyridinophane (O_2 -L), **4**. First, 11.56 g (37) mmol) of lithium salt 8 was dissolved in 120 mL of dry 1,3-dimethyl-2-imidazolidinone (DMI) in a 250 mL round-bottomed flask followed by the addition of 5.93 g (40 mmol) of 2,6-dichloropyridine. The mixture was sealed under argon and heated at 185 °C for 3 days before being cooled to room temperature and quenched by excess aqueous KOH solution. The mixture was combined with 500 mL of water and extracted with 50 mL of dichloromethane three times. After removal of dichloromethane using a rotavap, the residue was distilled at 110 °C under high vacuum to remove DMI and then at 230 °C (0.1 mmHg) to collect crude product 4, which was further purified by recrystallization in EtOAc and hexanes. The pure macrocycle is a white crystalline solid (1.31 g, 11%), producing crystals suitable for single crystal X-ray diffraction. ¹H NMR (600 MHz, CDCl₃, 22 °C), δ: 7.76 (t, J = 7.9 Hz, 1H), 7.46 (t, J = 7.7 Hz, 2H), 6.81 (dd, J = 7.5, 0.8 Hz, 2H), 6.76 (d, J = 7.9 Hz, 2H), 6.68 (dd, J = 7.9, 0.8 Hz, 2H), 3.24 (s, 4H). ¹³C NMR (126 MHz, CDCl₃, 22 °C), δ: 161.72, 161.20, 158.63, 142.29, 139.21, 119.44, 111.06, 106.63, 35.82. ESI-MS calcd. for C₁₂H₁₁Cl₂N₂⁺ [M + H]⁺ 292.11. Found: 292.20.

Preparation of Dichloropalladium(II) Complex 9. First, 30.0 mg of $PdCl_2$ was suspended in 3 mL of dry acetonitrile in a 10 mL Schlenk tube. The mixture was sealed and heated at 85 °C for 1 h until all solids disappeared. The solution was cooled to room temperature, and 55.0 mg of 4 was added. The reaction was heated at 50 °C for an additional 2 h followed by slow cooling to 0 °C. The product separated from the solution as reddish powder and was collected by filtration. The powder was dried under high vacuum to give 80 mg (94%) of pure 9. Then, 9 mg of the product was dissolved in 15 mL of DCM in an Erlenmeyer flask and sealed in a bottle containing 30 mL of pentanes. In a week, crystals were produced suitable for single-crystal characterization. ¹H NMR (500 MHz, CD₂Cl₂, -40 °C), δ : 8.06 (t, J = 8.1 Hz, 1H), 8.02 (t, J = 7.8 Hz, 1H), 7.95 (t, J = 7.9 Hz, 1H), 7.39 (d, J = 8.0 Hz, 1H), 7.33 (q, J = 7.8, 7.3

Hz, 3H), 7.13 (d, J = 8.2 Hz, 1H), 7.09 (d, J = 8.2 Hz, 1H), 4.17 (t, J = 12.1 Hz, 1H), 3.50–3.40 (m, 1H), 3.37 (t, J = 11.8 Hz, 1H), 2.55 (t, J = 12.0 Hz, 1H). 1 H NMR (400 MHz, CD₂Cl₂, 22 $^\circ$ C), δ: 8.12 (t, J = 8.0 Hz, 1H), 7.98 (t, J = 7.8 Hz, 2H), 7.35 (dd, J = 7.6, 1.1 Hz, 2H), 7.24 (t, J = 7.1 Hz, 3H), 4.15 (s, 2H), 3.17 (s, 2H). ESI-MS calcd. for $C_{17}H_{14}Cl_2N_3O_2Pd^+$ [M + H] $^+$ 467.95. Found: 467.97.

Preparation of Chlorocopper(I) Complex 10. In a glovebox, an oven-dried 5 mL round-bottomed flask was charged with 10.0 mg of CuCl, 29.6 mg of 4, and 1 mL of anhydrous degassed dichloromethane. The mixture was stirred at room temperature for 10 min, and the product was formed quantitatively to give a yellowish solution. Complex **10** could be isolated as a yellow solid upon removal of dichloromethane and drying under high vacuum. ¹H NMR (400 MHz, CD₂Cl₂, 22 °C), δ : 7.92 (t, J = 7.9 Hz, 1H), 7.79 (t, J = 8.1 Hz, 2H), 7.52–6.18 (m, 6H), 3.62 (s, 4H). ¹³C NMR (CD₂Cl₂, 22 °C), δ : 36.0, 106.9, 113.1, 121.1, 140.7, 144.1, 157.5, 158.2, 159.8.

Attempted Preparation of Platinum(II) Complexes. Stirring mixture of aqueous K_2PtCl_4 and 4 in did not lead to any changes after 2 days at 22 °C. Similarly, no changes were observed when a mixture of 4 and $Pt_2Me_4(SMe_2)_2$ was kept in THF solution after 1 day at 22 °C.

General Procedure for Aziridination of Olefins with PhINTs Catalyzed by 10 or 10/NaBAr^F₄. First, 37.3 mg of PhINTs, 3.00 or 5.00 equiv of the olefin substrate, and 0.6 mL of degassed anhydrous dichloromethane were charged to an oven-dried NMR Young tube under the protection of Ar. The Young tube was gently shaken to make a suspension before being cooled to 0 °C in ice/water bath. Then, 0.2 mL of a 25 mM solution of 10 or a solution produced by stirring 25 mM 10 with solid NaBArF4 in dry dichloromethane was injected into the Young tube. The color of the mixture changed to deep green immediately. The tube was removed periodically from the ice bath and briefly shaken. After 5-15 min, all solids have dissolved to produce a clear solution so signifying the end of the reaction. Yields of the aziridines were determined by ¹H NMR integration of the resulting sharp spectra using 1,4-dioxane (see Figure S14) or 4,4'bis(tert-butyl)biphenyl as an internal standard added to reaction mixtures after the reactions were complete. Using this technique, we have found that formation of PhI was quantitative, based on the amount of PhINTs used, as observed for various other pyridine-supported Cu-based catalysts. ¹⁶ To confirm the identity of resulting aziridines, the reaction solutions were passed through a short column filled with alumina, and the products were eluted with CH2Cl2. The resulting liquids were taken to dryness, and all volatiles were removed under high vacuum using a warm water bath. ¹H NMR parameters of the isolated products 14-24 (see below) matched well to those

N-(*p*-Toluenesulphonyl)-9-azabicyclo[6.1.0]nonane, 14.²⁴ ¹H NMR (CDCl₃, 22 °C), δ: 1.17–1.61 (m, 10H), 1.93–2.02 (m, 2H), 2.40 (s, 3H), 2.74 (m, 2H), 7.29 (d, ${}^{3}J_{\rm H-H}$ = 8.4 Hz, 2H), 7.77 (d, ${}^{3}J_{\rm H-H}$ = 8.4 Hz, 2H).

N-(*p*-Toluenesulphonyl)-8-azabicyclo[5.1.0]octane, 15.²⁴ ¹H NMR (CDCl₃, 22 °C), δ: 1.24–1.12 (m, 1H), 1.62–1.40 (m, 5H), 1.90–1.76 (m, 4H), 2.44 (s, 3H), 2.98–2.92 (m, 2H), 7.32 (d, J = 8.3 Hz, 2H), 7.82 (d, J = 8.3 Hz, 2H).

N-(p-Toluenesulphonyl)-7-azabicyclo[4.1.0]heptane, 16.. 24,25 1 H NMR (CDCl $_{3}$, 22 $^{\circ}$ C), δ: 1.15–1.25 (m, 2H), 1.32–1.42 (m, 2H), 1.72–1.80 (m, 4H), 2.42 (s, 3H), 2.95 (m, 2H), 7.30 (d, 3 J_{H-H} = 8.4 Hz, 2H), 7.79 (d, 3 J_{H-H} = 8.4 Hz, 2H).

N-(*p*-Toluenesulphonyl)-6-azabicyclo[3.1.0]hexane, 17.²⁶ ¹H NMR (CDCl₃, 22 °C), δ: 1.50–1.67 (m, 4H), 1.87–1.97 (m, 2H), 2.43 (s, 3H), 3.31 (brs, 2H), 7.30 (d, $^3J_{\rm H-H}$ = 8.2 Hz, 2H), 7.79 (d, $^3J_{\rm H-H}$ = 8.2 Hz, 2H).

2-Phenyl-N-tosylaziridine, 18..^{23,24,26} ¹H NMR (CDCl₃, 22 °C), δ : 2.38 (d, J = 4.5 Hz, 1H), 2.43 (s, 3H), 2.98 (d, J = 8 Hz, 1H), 3.77 (dd, J = 8, 4.5 Hz, 1H), 7.31–7.19 (m, 5H), 7.33 (d, J = 8 Hz, 2H), 7.87 (d, J = 8 Hz, 2H).

2,2,3-Trimethyl-*N***-tosylaziridine, 19.**⁸ ¹H NMR (CDCl₃, 22 °C), δ : 1.12 (d, ${}^{3}J_{\rm H-H}$ = 5.8 Hz, 3H), 1.26 (s, 3H), 1.67 (s, 3H), 2.42 (s, 3H), 2.94 (q, ${}^{3}J_{\rm H-H}$ = 5.8 Hz, 1H), 7.32 (d, ${}^{3}J_{\rm H-H}$ = 8.4 Hz, 2H), 7.77 (d, ${}^{3}J_{\rm H-H}$ = 8.4 Hz, 2H).

2,2,3,3-Tetramethyl-*N***-tosylaziridine, 20.**²⁷ ¹H NMR (CD₂Cl₂, 22 °C), δ : 1.45 (s, 12H), 2.42 (s, 3H), 7.31 (d, ${}^{3}J_{\rm H-H}$ = 8.4 Hz, 2H), 7.77 (d, ${}^{3}J_{\rm H-H}$ = 8.4 Hz, 2H).

2-Carbomethoxy-*N***-tosylaziridine, 21.** ^{28 1}H NMR (CDCl₃, 22 °C), δ : 2.42 (s, 3H), 2.53 (d, ${}^{3}J_{\rm H-H}$ = 4.1 Hz, 1H), 2.73 (d, ${}^{3}J_{\rm H-H}$ = 7.3 Hz, 1H), 3.31 (dd, ${}^{3}J_{\rm H-H}$ = 4.1 Hz, ${}^{3}J_{\rm H-H}$ = 7.1 Hz, 1H), 7.32 (d, ${}^{3}J_{\rm H-H}$ = 8.1 Hz, 2H), 7.81 (d, ${}^{3}J_{\rm H-H}$ = 8.0 Hz, 2H).

2-Carbomethoxy-2-methyl-N-tosylaziridine, 22.²⁹ ¹H NMR (CDCl₃, 22 °C), δ : 1.87 (s, 3H), 2.41 (s, 3H), 2.68 (s, 3H), 2.76 (s, 3H), 7.30 (d, ${}^{3}J_{\rm H-H} = 8.2$ Hz, 2H), 7.81 (d, ${}^{3}J_{\rm H-H} = 8.3$ Hz, 2H). **2-tert-Butyl-N-tosylaziridine, 23.**³⁰ ¹H NMR (CD₂Cl₂, 22 °C),

2-tert-Butyl-N-tosylaziridine, 23. ³ ¹H NMR (CD₂Cl₂, 22 °C), δ : 0.78 (s, 9H), 2.18 (d, J = 4.2 Hz, 1H), 2.42 (m, 1H), 2.43 (s, 3H), 2.47–2.52 (m, 1H), 7.30 (d, ${}^{3}J_{H-H}$ = 8.4 Hz, 2H), 7.80 (d, ${}^{3}J_{H-H}$ = 8.4 Hz, 2H).

2-neo-Pentyl-N-(p-toluenesulphonyl)-aziridine, 24. ¹⁶ ¹H NMR (CDCl₃, 22 °C), δ : 0.90 (s, 9H), 1.25 (m, 1H), 1.45 (m, 1H), 1.94 (d, ${}^{3}J_{\rm H-H}$ = 4.6 Hz, 1H), 2.41 (s, 3H), 2.57 (d, ${}^{3}J_{\rm H-H}$ = 7.0 Hz, 1H), 2.78 (m, 1H), 7.30 (d, ${}^{3}J_{\rm H-H}$ = 8.4 Hz, 2H), 7.79 (d, ${}^{3}J_{\rm H-H}$ = 8.4 Hz, 2H).

CONCLUSION

New dioxa-[2.1.1]-(2,6)-pyridinophane ligand 4 was synthesized, and its dichloropalladium(II) and chlorocopper(I) complexes were prepared. Both the palladium and copper complexes contain κ^2 -N₁N-coordinated pyridinophane 4. In palladium complex 9, ligand 4 is bound to the metal through symmetry-nonequivalent pyridine fragments to avoid electron repulsion between its third nitrogen donor lone pair and the metal d_{z^2} electrons. That results in a C_1 symmetry of the complex in solid state and in CH₂Cl₂ solutions at −40 °C. In turn, the copper complex 10 has an idealized C_s symmetry in the solid state and in solutions with the metal atom avoiding coordination to the electron-poorest pyridine fragment which has two bridging oxygen atoms attached. Both metal complexes are fluxional at 22 °C. Some unusual ¹H NMR patterns exhibited by 10 could be interpreted as a result of a fast intermolecular Cu^ICl fragment exchange between different macrocyclic ligands. Overall, new ligand 4 is a poor donor of electrons and forms much weaker metal complexes, as compared to corresponding CH2-bridged ligand 1. The electron-poor nature of 4 and derived coordination compounds appears to be advantageous for processes involving strongly oxidizing conditions such as nitrene transfer. A catalyst derived from chlorocopper(I) complex supported by the new ligand performs well in olefin aziridination with PhINTs as a nitrene source and is somewhat superior, as compared to its CH2-bridged analog, 11. Further characterization of catalysts derived from 10 and similar complexes in oxidative functionalization reactions may represent a particular future interest.

ASSOCIATED CONTENT

S Supporting Information

The Supporting Information is available free of charge on the ACS Publications website at DOI: 10.1021/acs.inorg-chem.9b02618.

NMR spectra and computational details (PDF)

Accession Codes

CCDC 1935653, 1935654, and 1947056 contain the supplementary crystallographic data for this paper. These data can be obtained free of charge via www.ccdc.cam.ac.uk/data_request/cif, or by emailing data_request@ccdc.cam.ac.uk, or by contacting The Cambridge Crystallographic Data

Centre, 12 Union Road, Cambridge CB2 1EZ, UK; fax: +44 1223 336033.

AUTHOR INFORMATION

Corresponding Author

*E-mail: avederni@umd.edu.

ORCID ®

Jiaheng Ruan: 0000-0003-0907-5685

Andrei N. Vedernikov: 0000-0002-7371-793X

Notes

The authors declare no competing financial interest.

ACKNOWLEDGMENTS

This work was supported by the National Science Foundation (CHE-1464772 and CHE-1800089) and, in part, the US—Israel Binational Science Foundation (grant 2014254).

REFERENCES

- (1) Barefield, E. K.; Lovecchio, F. V.; Tokel, N. E.; Ochiai, E.; Busch, D. H. Synthesis, Properties, and Electrochemical Studies of a Series of Nickel(II) Complexes with Related Macrocyclic Ligands of Varied Unsaturation. *Inorg. Chem.* 1972, 11, 283–288.
- (2) Ribas, X.; Jackson, D. A.; Donnadieu, B.; Mahía, J.; Parella, T.; Xifra, R.; Hedman, B.; Hodgson, K. O.; Llobet, A.; Stack, T. D. P. Aryl C–H activation by Cu^{II} to form an Organometallic Aryl–Cu^{III} Species: a Novel Twist on Copper Disproportionation. *Angew. Chem., Int. Ed.* **2002**, *41*, 2991–2994.
- (3) (a) Brietzke, T.; Dietz, T.; Kelling, A.; Schilde, U.; Bois, J.; Kelm, H.; Reh, M.; Schmitz, M.; Koerzdoerfer, T.; Leimkuehler, S.; et al. The 1,6,7,12-Tetraazaperylene Bridging Ligand as an Electron Reservoir and Its Disulfonato Derivative as Redox Mediator in an Enzyme–Electrode Process. *Chem. Eur. J.* 2017, 23, 15583–15587. (b) Koch, W. O.; Krueger, H.-J. A Highly Reactive and Catalytically Active Model System for Intradiol-Cleaving Catechol Dioxygenases: Structure and Reactivity of Iron(III) Catecholate Complexes of N,N'-Dimethyl-2,1 l-diaza[3.3](2,6)pyridinophane. *Angew. Chem., Int. Ed. Engl.* 1996, 34, 2671–2674.
- (4) Fuchigami, K.; Rath, N. P.; Mirica, L. M. Mononuclear Rhodium(II) and Iridium(II) Complexes Supported by Tetradentate Pyridinophane Ligands. *Inorg. Chem.* **2017**, *56*, 9404–9408.
- (5) (a) Vedernikov, A. N.; Huffman, J. C.; Caulton, K. G. [n.1.1]-(2,6)-Pyridinophanes: A New Ligand Type Imposing Unusual Metal Coordination Geometry. *Inorg. Chem.* **2002**, *41*, 6867–6874. (b) Vedernikov, A. N.; Pink, M.; Caulton, K. G. Design and Synthesis of Tridentate Facially Chelating Ligands of [2.n.1]-(2,6)-Pyridinophane Family. *J. Org. Chem.* **2003**, *68*, 4806–4814.
- (6) Vedernikov, A. N.; Pink, M.; Caulton, K. G. Influence of the [2.1.1]-(2,6)-Pyridinophane Macrocycle Ring Size Constraint on the Structure and Reactivity of Copper Complexes. *Inorg. Chem.* **2004**, *43*, 4300–4305.
- (7) (a) Vedernikov, A. N.; Huffman, J. C.; Caulton, K. G. [2.1.1]-(2,6)-pyridinophane(L)-Controlled Alkane C-H Bond Cleavage: (L)PtMe₂H⁺ as a Precursor to the Geometrically "Tense" Transient (L)PtMe⁺. New J. Chem. 2003, 27, 665–667. (b) Vedernikov, A. N.; Caulton, K. G. Control of H-C(sp³) Bond Cleavage Stoichiometry: Clean Reversible Alkyl Ligand Exchange with Alkane in LPt(Alk)-(H)₂⁺ (L = [2.1.1]-(2,6)-Pyridinophane). Angew. Chem., Int. Ed. 2002, 41, 4102–4104. (c) Vedernikov, A. N.; Caulton, K. G. N-Pt^{IV}-H/N-H-Pt^{II} Intramolecular Redox Equilibrium in a Product of H-C(sp²) Bond Cleavage and Unusual Alkane/Arene CH Bond Selectivity of Transient PtR(L)⁺ Species. Chem. Commun. 2003, 358–359. (d) Vedernikov, A. N.; Pink, M.; Caulton, K. G. Hydrocarbyl Ligand "Tuning" of the Pt^{II/IV} Redox Potential. Inorg. Chem. 2004, 43, 3642–3646.

(8) Vedernikov, A. N.; Caulton, K. G. Angular Ligand Constraint Yields an Improved Olefin Aziridination Catalyst. *Org. Lett.* **2003**, *5*, 2591–2594.

- (9) Pappalardo, S.; Bottino, F.; Di Grazia, M.; Finocchiaro, P.; Mamo, A. A Versatile One-pot Synthesis of Symmetrical *N*-Tosylazamacrocycles. *Heterocycles* **1985**, 23, 1881–1884.
- (10) (a) Castro, G.; Bastida, R.; Macías, A.; Pérez-Lourido, P.; Platas-Iglesias, C.; Valencia, L. Pyridinophane Platform for Stable Lanthanide(III) Complexation. *Inorg. Chem.* **2013**, *52*, 6062–6072. (b) Castro, G.; Bastida, R.; Macías, A.; Pérez-Lourido, P.; Platas-Iglesias, C.; Valencia, L. Lanthanide(III) Complexation with an Amide Derived Pyridinophane. *Inorg. Chem.* **2015**, *54*, 1671–1683.
- (11) Vedernikov, A. N.; Caulton, K. G. Facile Alkane Functionalization in Copper-[2.1.1]-(2,6)-pyridinophane-PhINTs Systems. *Chem. Commun.* **2004**, 162–163.
- (12) Moegling, J.; Hoffmann, A.; Thomas, F.; Orth, N.; Liebhäuser, P.; Herber, U.; Rampmaier, R.; Stanek, J.; Fink, G.; Ivanović-Burmazović, I.; Herres-Pawlis, S. Designed To React: Terminal Copper Nitrenes and Their Application in Catalytic C–H Aminations. *Angew. Chem., Int. Ed.* **2018**, *57*, 9154–9159.
- (13) Gava, R.; Olmos, A.; Noverges, B.; Varea, T.; Álvarez, E.; Belderrain, T. R.; Caballero, A.; Asensio, G.; Pérez, P. J. Discovering Copper for Methane C—H Bond Functionalization. *ACS Catal.* **2015**, *5*, 3726—3730.
- (14) Here is a rare exception of a Cu(II) complex derived from an electron-poor pyridinophane ligand: Newkome, G. R.; Joo, Y. J.; Evans, D. W.; Fronczek, F. R.; Baker, G. R. l,3,5-Tri[2,6]-pyridacyclohexaphane-2,4,6-trione Ketals: Synthesis, Structural Analysis, and Complexation. *J. Org. Chem.* **1990**, *55*, 5714–5719.
- (15) (a) Meneghetti, S. P.; Lutz, P. J.; Kress, J. Neutral and Cationic Palladium(II) Complexes of a Diazapyridinophane. Structure, Fluxionality, and Reactivity toward Ethylene. *Organometallics* **2001**, 20, 5050–5055. (b) Khusnutdinova, J. R.; Luo, J.; Rath, N. P.; Mirica, L. M. Late First-Row Transition Metal Complexes of a Tetradentate Pyridinophane Ligand: Electronic Properties and Reactivity Implications. *Inorg. Chem.* **2013**, *52*, 3920–3932.
- (16) Mohr, F.; Binfield, S.; Fettinger, J. C.; Vedernikov, A. N. A practical, Fast and High-yielding Aziridination Procedure Using Simple Cu(II) Complexes Containing N-Donor Pyridine-based Ligands. J. Org. Chem. 2005, 70, 4833–4839.
- (17) Dauban, P.; Dodd, R. H. Application of the Evans Aziridination Procedure to 2-Substituted Acrylates and Cinnamates: An Expedient Route to α -Substituted α and β -Amino Acids. *Tetrahedron Lett.* **1998**, 39, 5739–5742.
- (18) Mona, C. E.; Besserer-Offroy, E.; Cabana, J.; Leduc, R.; Lavigne, P.; Heveker, N.; Marsault, E.; Escher, E. Design, synthesis, and biological evaluation of CXCR4 ligands. *Org. Biomol. Chem.* **2016**, *14*, 10298–10311.
- (19) Li, Y.; Diebl, B.; Raith, A.; Kühn, F. E. Syntheses of acetonitrile ligated copper complexes with perfluoroalkoxy aluminate as counter anion and their catalytic application for olefin aziridination. *Tetrahedron Lett.* **2008**, *49*, 5954–5956.
- (20) Parr, R. G.; Yang, W. Density-Functional Theory of Atoms and Molecules; Oxford University Press: Oxford, U.K., 1989.
- (21) Perdew, J. P.; Burke, K.; Ernzerhof, M. Generalized gradient approximation made simple. *Phys. Rev. Lett.* **1996**, *77*, 3865–3868.
- (22) Jaguar, version 8.4, Schrödinger, LLC, New York, NY, 2014.
- (23) Perez, P. J.; Brookhart, M.; Templeton, J. L. A Copper(I) Catalyst for Carbene and Nitrene Transfer to Form Cyclopropanes, Cyclopropenes, and Aziridines. *Organometallics* **1993**, *12*, 261–262.
- (24) Yoshimura, A.; Nemykin, V. N.; Zhdankin, V. V. o-Alkoxyphenyliminoiodanes: Highly Efficient Reagents for the Catalytic Aziridination of Alkenes and the Metal-Free Amination of Organic Substrates. *Chem. Eur. J.* 2011, 17, 10538–10541.
- (25) Chanda, B. M.; Vyas, R.; Bedekar, A. V. Investigations in the Transition Metal Catalyzed Aziridination of Olefins, Amination, and Other Insertion Reactions with Bromamine-T as the Source of Nitrene. *J. Org. Chem.* **2001**, *66*, 30–34.

(26) Hegedus, L. S.; McKearin, J. M. Palladium-catalyzed cyclization of omega.-olefinic tosamides. Synthesis of nonaromatic nitrogen heterocycles. *J. Am. Chem. Soc.* **1982**, *104*, 2444–2451.

- (27) Sugihara, Y.; Iimura, S.; Nakayama, J. Aza-pinacol rearrangement: acid-catalyzed rearrangement of aziridines to imines. *Chem. Commun.* **2002**, 134–135.
- (28) Evans, D. A.; Faul, M. M.; Bilodeau, M. T. Development of the Copper-Catalyzed Olefin Aziridination Reaction. *J. Am. Chem. Soc.* **1994**, *116*, 2742–2753.
- (29) Burgaud, B. G. M.; Horwell, D. C.; Padova, A.; Pritchard, M. C. Regioselective nucleophilic ring opening reactions of 2,2-disubstituted aziridines the asymmetric synthesis of α , α -disubstituted amino acids. *Tetrahedron* **1996**, *52*, 13035–13050.
- (30) Kawamura, K.; Fukuzawa, H.; Hayashi, M. Novel *N,N,P*-Tridentate Ligands for the Highly Enantioselective Copper-Catalyzed 1,4-Addition of Dialkylzincs to Enones. *Org. Lett.* **2008**, *10*, 3509–3512.